Evaluation of two thin CT dose profile detectors and a new way to perform QA in a CTDI head phantom

Master Degree Thesis in Radiation Physics

Björn Cederquist

Supervisors: Lars Herrnsdorf, Simone Eriksson,
Magnus Båth, Jonny Hansson

Department of Radiation Physics
Göteborg University
Göteborg, Sweden 2008

Abstract

In this thesis project two similar detectors for measurements of dose profile and dose from computed tomography (CT) have been evaluated. A new and faster way of quality assurance with the detectors has been evaluated.

It is shown that the detectors can measure dose profiles using helical scans. This makes it possible to measure the whole dose profile quickly by using the CT table movement.

Measurements have been made in more than one phantom to examine the increase of scattered radiation.

The detectors can show how much dose that is underestimated with $CTDI_{100}$ compared to CTDI. The amount of underestimated radiation appears to increase, as the beam collimation is getting wider with newer cone beam based MDCT.

The new way of quality assurance makes it possible to get a lot of dosimetric parameters with just one helical measurement in a CTDI head phantom.

Table of contents

1. Introduction

Medical x-ray is the largest contributor to of radiation exposure to the population from artificial sources [1]. Computed Tomography (CT) contributes with 70 % of that radiation [2]. About 660,000 CT examinations are done in Sweden every year [3]. A CT examination gives 10-50 times more dose to a patient than thecorresponding conventional x-ray examination [4]. Hence it is important that quality controls are made regularly to ensure that the CT system performs well.

The absorbed dose to a patient is the result of both primary radiation and scattered radiation from surrounding tissues. For quality assurance (QA), measurements of the dose from CT are performed in a phantom in order to include internal scattered radiation within the body. Dose measurements are primarily done with a 100 mm long pencil ion chamber. Its active volume is insufficient to collect all the scattered radiation. As beam collimation (the nominal beam width in the z direction in this thesis) is getting larger than 100 mm, not even all the primary radiation can be measured with this method. At present, a beam collimation of 160 mm is available (Toshiba Aquilion ONE, Tochigi, Japan). The dose profile, which is the dose distribution along the axis of rotation, can be measured by using an array of thermo luminescent dosimeters (TLD), optically stimulated luminescence (OSL) [5] or x-ray film. TLD is a time consuming and expensive method, OSL is time consuming and x-ray films are disappearing from many hospitals due to the advent of digital imaging. It would be preferable to have all the dose information from one single measurement independent of the beam collimation.

New techniques are becoming available for CT QA. In this work an old and a new semiconductor detector from RTI Electronics AB, called the Computed Tomography Slice Detector D2 (CT-SDD2) and the Computed Tomography Slice Detector D2 (2x2) (CT-SDD2 (2x2)), have been evaluated. A new method for CT QA with the detectors has also been developed and evaluated.

1.1 Basic Information on CT

CT is a method to create 3D images of a certain volume of a body. By irradiating with a fan-beam from an x-ray tube in one rotation, around the body, and collecting the radiation that has been modulated according to the body anatomy, an image of that plane in the volume can be reconstructed (Figure 1). The thickness of the fan-beam depends on the primary collimators (Figure 1 b)). To shorten the scanning time several detector rows have been employed so that more than one image per rotation may be obtained. The method is called multi-detector row CT (MDCT) and with this method the beam collimation is getting larger. The geometry of the fan-beam then looks more and more like a cone-beam.

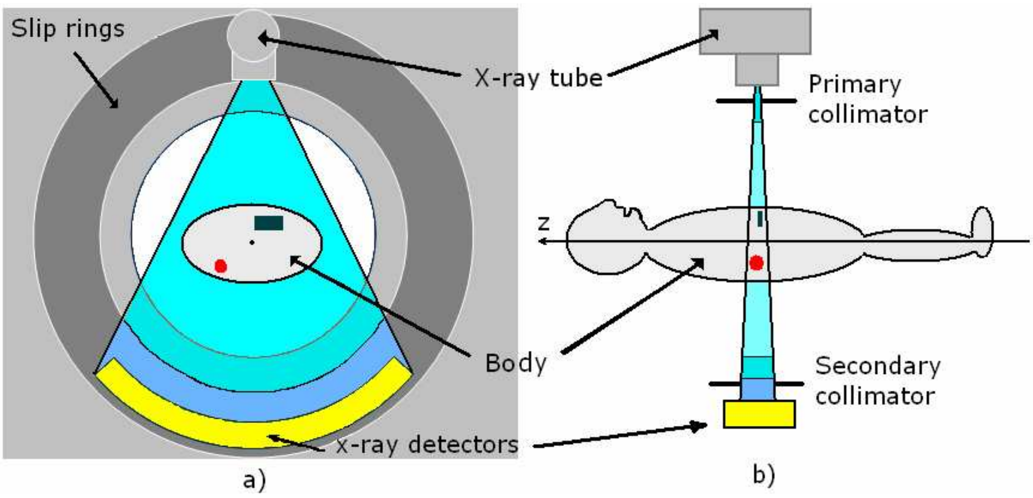

Figure 1: The principle of a CT seen from a) the front and b) from the side. z is the axis of rotation.

The first CT only used axial sequential scans (Figure 2 a)) but during the last 20 years CT systems can use a spiral function. This means that the body is moved continuously through the gantry of the CT while it is irradiating (Figure 2 b)). The motion of the x-ray tube and the detectors as seen from the gantry center is that of a spiral rotation path around the body. The projection data needed for reconstruction of axial images can be obtained by interpolation of the collected data.

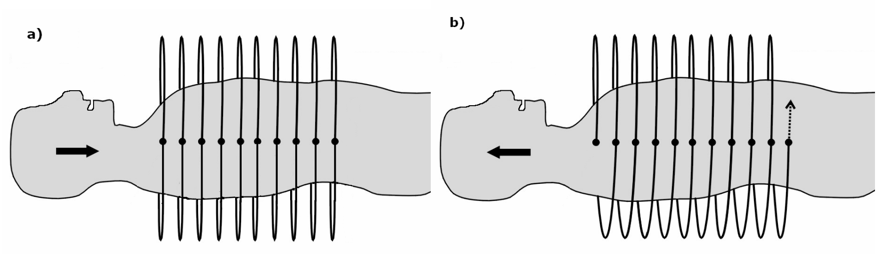

Figure 2: a) Axial sequential scan, b) Helical scan

1.2 Dosimetry

1.2.1 Dose profile

The dose profile (Figure 3 a)) is the dose distribution along the central axis (z-axis) or parallel to the axis of rotation. It is affected e.g. by the primary collimators, the distance between the collimation and the x-ray tube, the penumbra and by the scattered radiation. It can be measured both in air and in a phantom.

An ideal dose profile would have the shape of a rectangular block that is exactly as wide as the beam collimation Nd (Figure 3 a)) set on the CT console. Unfortunately such a dose profile is impossible to achieve due to the scattered radiation and geometrical conditions. A commonly used measure of the dose distribution is the full width at half maximum (FWHM) of the dose profile [6].

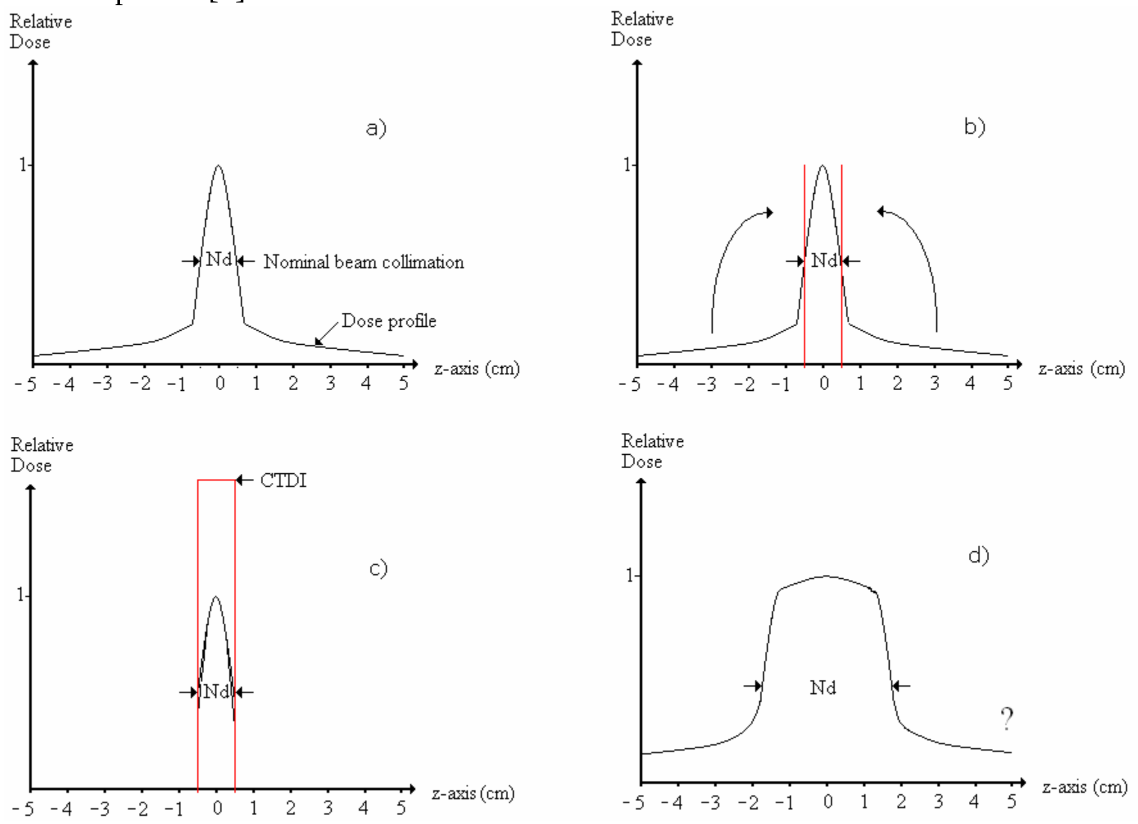

Figure 3: a) Dose profile for a 10 mm beam collimation measured in a phantom, b) The term CTDI is the whole dose in the profile so if all dose is put inside the nominal beam collimation c) it illustrates the CTDI, d) Dose profile for a 40 mm beam collimation measured in a phantom (Figure 5).

1.2.2 Pitch

Pitch is defined as the speed of the patient table T multiplied by the time per rotation F divided by the number of simultaneously acquired images N and the nominal image thickness d [7]:

$$p = \frac{TF}{Nd} \quad . \qquad (1)$$

Pitch values < 1 are indicators of overlapping and pitch values > 1 are indicators for low-dose scanning mode when the same scan parameters are used (Figure 4).

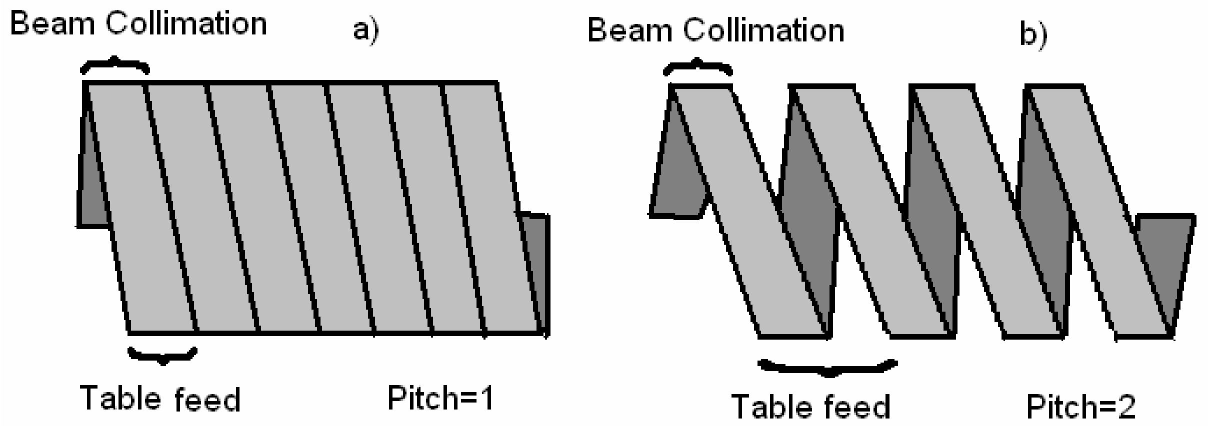

Figure 4: Illustration of helical scans with a) pitch 1 and b) pitch 2.

1.2.3 CTDI

The fundamental dose quantity from a CT system is called Computed Tomography Dose Index (CTDI). For one axial scan CTDI is defined as the integral of the dose profile along the rotational axis of the CT (z-axis) (Figure 5) divided by the total nominal beam collimation N·d [6]:

$$CTDI = \int_{-\infty}^{+\infty} \frac{D(z)}{Nd} dz \text{ [mGy].} \qquad (2)$$

D(z) is the dose at a certain point z on the z-axis. The total nominal beam collimation N·d is the number of simultaneously acquired images N multiplied with the nominal image thickness d.

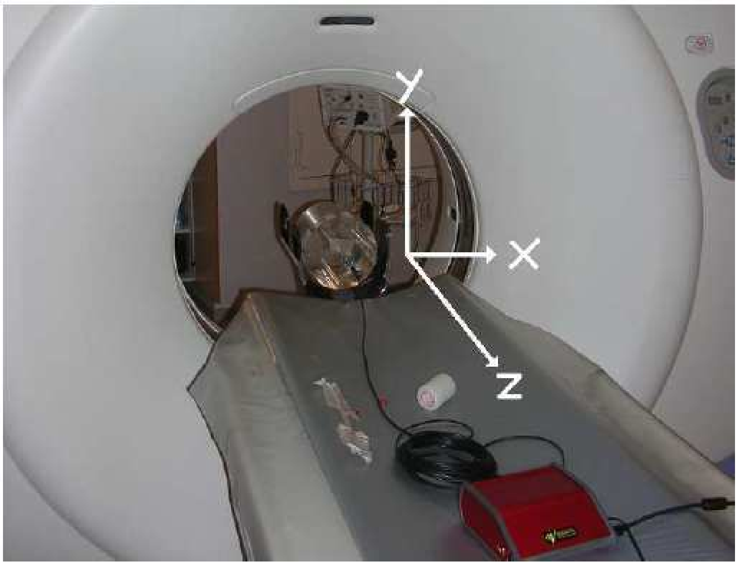

Figure 5: CT-SDD2 in a head phantom in a CT. The line z is parallel to the axis of rotation.

One way to interpret CTDI is to imagine the entire dose being deposited into a rectangular profile with the same width as the nominal beam collimation (Figure 3 b) and 3 c)). The dose within the rectangular profile is the CTDI [6].

To integrate CTDI from -∞ to +∞ is not practically possible. A common limit is to integrate over a length of a 100 mm which results in $CTDI_{100}$ [6]:

$$CTDI_{100} = \int_{-50}^{+50} \frac{D(z)}{Nd} dz \text{ [mGy].} \qquad (3)$$

The term weighted CTDI, $CTDI_w$, is used to get an indication of the average $CTDI_{100}$ in a cross section of a phantom [6]:

$$CTDI_w = \frac{1}{3} CTDI_{100,c} + \frac{2}{3} CTDI_{100,p} \text{ [mGy].} \qquad (4)$$

$CTDI_{100,c}$ is $CTDI_{100}$ in the center and $CTDI_{100,p}$ is the mean $CTDI_{100}$ from the several peripheral holes. The phantoms used are CTDI phantoms of polymethylmetacrylate (PMMA) with a diameter of 160 mm for head and 320 mm for body according to the European Quality Guidelines for CT QA [8].

It is enough to integrate the dose over 100 mm when measurements are performed free in air but not in a phantom. The measured $CTDI_{100}$ in a phantom is known to be an underestimation of CTDI but with beam collimation around 10 mm the underestimated dose is known to be constant. Today the beam collimation becomes wider and wider. The amount of dose that is not measured with $CTDI_{100}$ in a phantom at a beam collimation of 40 mm may be increasing compared to 10 mm, (illustrated in Figure 3 d)).

The average dose to the whole volume made by a series of scans is called $CTDI_{vol}$. For helical scans it is calculated by dividing $CTDI_w$ by the pitch [2]:

$$CTDI_{vol} = \frac{CTDI_w}{p} \text{ [mGy].} \qquad (5)$$

For axial sequential scans it is calculated by multiplying the CTDIw by the nominal beam collimation Nd and dividing it by the increment I between the scans of the series [2]:

$$CTDI_{vol} = \frac{Nd}{I} CTDI_w \text{ [mGy].} \qquad (6)$$

1.2.4 MSAD and DLP

When multiple rotations are performed, the dose profiles will overlap (Figure 6). The increased average dose value in the central slice is called the Multiple Scan Average Dose (MSAD) [7].The area under the MSAD curve is called the Dose Length Product (DLP) and represents the complete radiation exposure, i.e. the integral effect of the scan. The definition of DLP is the $CTDI_{vol}$ multiplied with the scan length L.

$$DLP = CTDI_{vol} \cdot L \text{ [mGy cm]} \qquad (7)$$

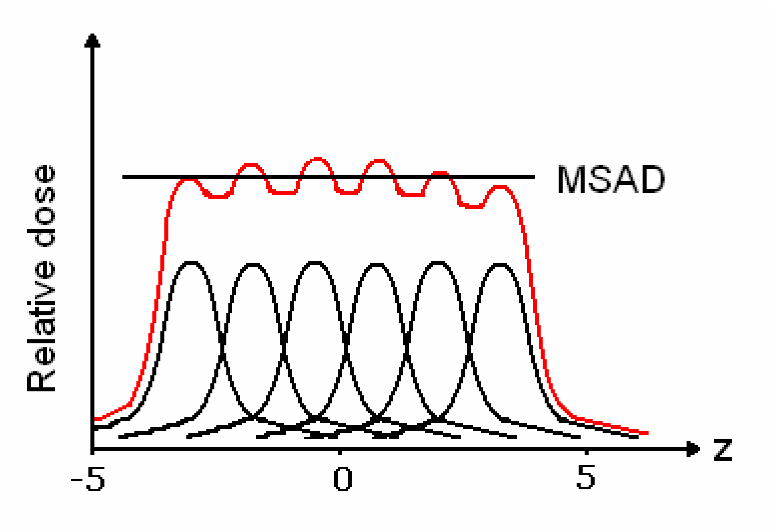

Figure 6: Illustration of MSAD. The area under the red curve illustrates the DLP

1.3 Computed Tomography Slice Detector

Before this thesis RTI Electronics AB had developed the computed tomography slice detector. Here follows its history so far.

The first idea of a CT slice detector started in the year 2003. It was a cylinder with two detectors separated by a distance of 100 mm [9]. Dose profile measured with the detector was made with helical scan mode and not single axial scan mode as for the TLD. A new probe was constructed in 2005 as a longer cylinder of polymethylmetacrylate (PMMA) with a thin aluminum shell (Figure 7 a)). The diameter of the cylinder was adapted to fit in a standard CTDI phantom i.e. 12.5 mm. The two identical detectors D1 and D2 were put in the end and in the middle of the probe. The distance between them was 160 mm in order to enable D1 to be outside the phantom while D2 was inside. This feature helped to avoid scattered radiation to reach the detector outside the radiation field, which would lead to an increase in the signal since the two detectors were connected electrically in parallel to the same out-signal. The name of the probe was CT-SD16 (Computed Tomography Slice Detector 16). The two-detector configuration was to enable measurement of the table speed and to use D1 as a "trig detector" for measuring the dose profile with D2. The thickness of the semiconductor detectors (PIN diodes) was 0.3 mm. They were placed standing on their ends so that the thin side was pointing in the direction of the radiation. On one side of the detectors, there was a back plane of high Z material such as tin, gold or silver to support and connect one side of the PIN diode. The back plane screened some of the radiation (Figure 7 b)). The PIN diode had fast linear radiation response [10] and could therefore easily track the dynamic variation of the dose rate in a helical scan. 2000 samples/second can be made, each with a 20 bits dynamic range, when the probe was connected to a Piranha or Barracuda electrometer [11]. A software, called "CT-SD16 1906", was written to handle all the data collected by the probe. The software "CT-SD16 1906" included a correction to compensate for the radiation that was attenuated unsymmetrically in z-direction due to the back plane.

To enable measurements with more than one phantom, detector D1 was removed so that it would not disturb by detecting scattered radiation in the same way as for the first detector which had a shorter distance between the detectors. The movement of the CT table was always very precise, hence measurement of the table speed was not really needed. The accuracy of table feed speed needed to be precise since the reconstruction software required this information to correct for the skewed data set. The software was improved using "manual trig" and therefore eliminated the need of a "trig detector". This probe was named CT-SDD2.

An advantage would be if the detector were very small so that it could be seen as a point detector with isotropic sensitivity. It would also be better if the detector did not have a back plane on one side. A new smaller detector (2x2 mm^2) specially designed to eliminate the unsymmetrical back plane attenuation was made as part of an EU research project "MÅL1" where RTI worked together with Mid Sweden University [12]. The probe containing this detector was called CT-SDD2 (2x2).

An illustration of how the probe was calibrated can be found in appendix A together with a calibration record. The energy dependence of the detector for heavy filtrated beams, as those inside a head or body phantom is not yet fully investigated. When compared to pencil ion chambers the probe have typically measured in the order of 10-20 % lower $CTDI_{100}$ than the CT chamber dependent of phantom used, type of pencil ion chamber used and actually calibration method. Since the calibration method is under investigation all measurements with the probe in this work are relative. Work to determine the energy dependence of the detector and some commonly used pencil ion chambers is going on [13] that hopefully will result in a calibration factor that more correctly can translate the measured signal to dose also in a phantom.

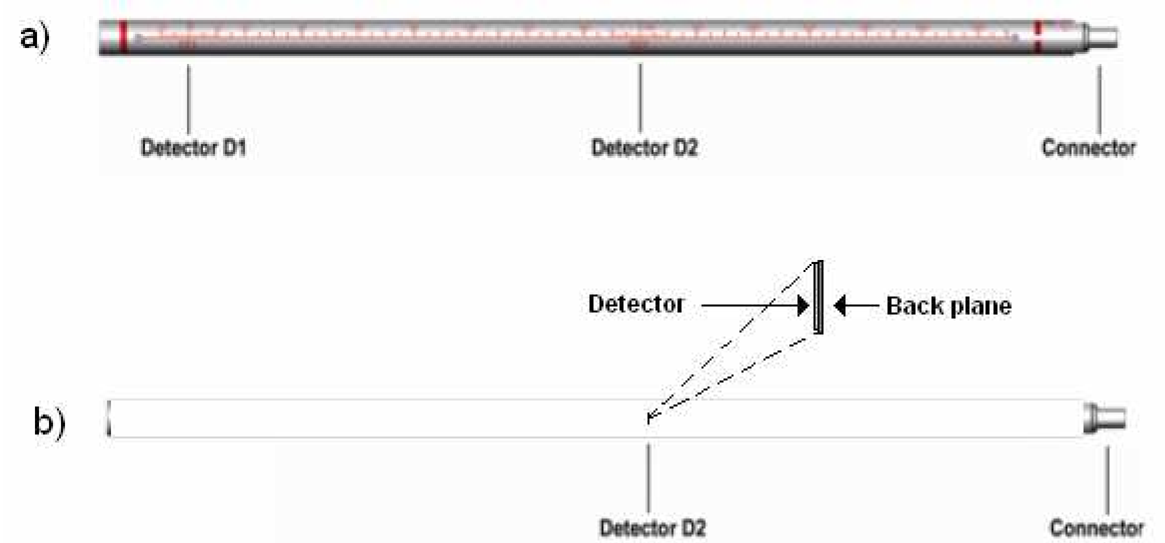

Figure 7: The design of a) the CT-SD16 and b) the CT-SDD2 in a cross-section.

1.4 Goals of study

The first goal was to see if it was possible to measure the same dose profile using helical scans and axial sequential scans, both in theory and in practice.

The second goal was to evaluate the dose profile measured with the CT-SDD2 and the CT-SDD2 (2x2). The CT-SDD2 (2x2) was to be compared to the liquid ion chamber (LIC) from Umeå University. The angular dependence and rotation symmetry for the CT-SDD2 (2x2) and the CT-SDD2 was also to be compared.

The third goal was to see how much $CTDI_{100}$ underestimates CTDI and how much it was underestimated with only one head phantom. A CTDI head phantom is only 15 cm long and most peoples' heads and necks are almost twice that length together.

Finally the forth goal was to develop and evaluate a new, easier and faster way of QA getting CTDI, $CTDI_{100}$, $CTDI_w$, $CTDI_{vol}$, DLP, FWHM and Scatter Index with just one helical measurement.

2. Materials and methods

2.1 Axial sequential scans versus helical scans

2.1.1 Method of measuring CTDI in helical mode

$CTDI_{100}$ is at present measured with a single axial scan on the centre of a 100 mm long pencil ion chamber. To measure $CTDI_{100}$ with helical scans with a small detector some changes must be made to the formalism of $CTDI_{100}$.

Based on the assumption that the dose rate in the measurement point is independent of the position of the tube, the dose from a whole rotation can be expressed as the signal Q per sample time t_s multiplied by the rotation time F and a calibration factor c which converts Q(z) to D(z).

$$D(z) = c\frac{Q(z)\cdot F}{t_s} \text{ [Gy].} \qquad (8)$$

Combining Equation 8 with Equation 2 leads to:

$$CTDI = \frac{1}{Nd}\int_{-\infty}^{\infty} D(z)dz = \frac{c}{Nd}\int_{-\infty}^{\infty}\frac{Q(z)\cdot F}{t_s}dz \text{ [Gy].} \qquad (9)$$

CT-SDD2 sample signals on its way through the radiation field. After every sampling time t_s and sampling length Δz, a signal Q_i is collected that represents the dose in that part of the z-axis. The integral can be changed to a sum of all signals per sampling time:

$$CTDI = c\frac{F}{Nd}\sum_i \frac{Q_i}{t_s}\Delta z \text{ [Gy].} \qquad (10)$$

Δz is the distance between two sample points and depends on the table speed T and the sampling time for a helical scan:

$$\Delta z = T \cdot t_s \text{ [m].} \qquad (11)$$

Combining Equation 11 with Equation 10 leads to:

$$CTDI = c\frac{FT}{Nd}\cdot t_s \sum_i \frac{Q_i}{t_s} \text{ [Gy].} \qquad (12)$$

Combining Equation 12 with Equation 1 leads to:

$$CTDI = pc\sum_i Q_i \text{ [Gy].} \qquad (13)$$

If n is the number of samplings within 100 mm:

$$n = \frac{100}{\Delta z}\ , \qquad (14)$$

then $CTDI_{100}$ is represented by:

$$CTDI_{100} = pc\sum_{i=1}^{n} Q_i \text{ [Gy].} \qquad (15)$$

Hence $CTDI_{100}$ can be measured with a helical scan if the collected signal ΣQ_i over the distance of 100 mm is multiplied with the calibration factor c and the pitch p. Measurements in the central hole in a phantom fulfils the earlier assumption of dose rate independent of the pitch. For measurements in the peripheral holes see 2.4.

2.1.2 Comparing helical scans with axial sequential scans

To see if a helical scan could get the same dose profile as axial sequential scans the CT-SDD2 (2x2) (S/N: 07030063) was put in a 30 cm long PMMA phantom with diameter of 160 mm. This phantom had a little bit bigger center hole than a standard CTDI-phantom. Some extra PMMA was put around the probe to fill the bigger hole. The head phantom was positioned free in air to prevent the dose profile from being disturbed by the table (Figure 8) and the scan parameters were 120 kV, 200 mA and 40 mm beam collimation on a GE LightSpeed VCT, Milwaukee, USA, at Norrlands University Hospital in Umeå. A helical scan was done on the phantom with a pitch of 0.984. Axial sequential scans were made on the phantom with 40 mm beam collimation by moving the table in small steps. A dose template in the software “CT-SD16 1906” was used to get signal for every axial sequential scan.

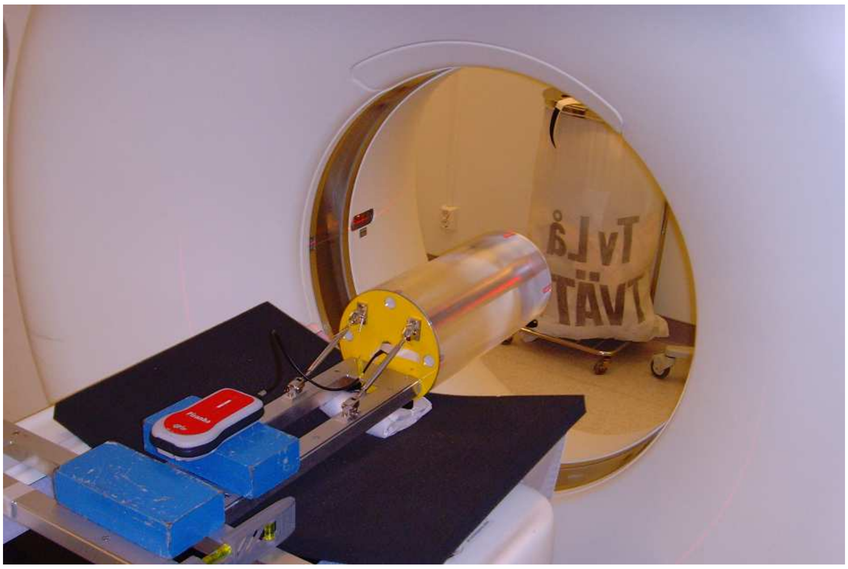

Figure 8: The CT-SDD2 (2x2) in a 30 cm long head phantom that was hanging outside the table.

2.2 Evaluation of the probe

2.2.1 Comparison of CT-SD D2 with CT-SDD2 (2x2)

The two types of CT-SDD2 had different detector size and configuration. To see how the correction for the back plane looked like for CT-SDD2 and to see if the dose profile from both detectors looked alike CT-SDD2 (S/N: 0601010) was put in the center hole on a standard CTDI head phantom. The phantom was placed on a neck support in a Siemens Somatom Sensation 16, Erlangen, Germany, at Sahlgrenska University Hospital (SU) in Göteborg and a helical scan was performed and the dose profile was measured. The scan parameters were 120 kV, 200 mA, 20 mm beam collimation and a pitch of 0.969. An identical measurement was performed with CT-SDD2 (2x2). Because of the different energy dependence between the two detectors and the lack of traceable calibration factors, the dose profiles were normalized to a peak value of 1 for comparison.

2.2.2 Comparison of CT-SDD2 (2x2) with a liquid ion chamber

An ordinary pencil ion chamber cannot create dose profiles. The liquid ion chamber (LIC) (S/N: CWH95-01) from Norrlands University Hospital in Umeå, Sweden, is able to measure dose profiles [14,15]. This could be a good reference chamber to CT-SDD2 (2x2) because of its identical detector length (0.3 mm) and the fact that its calibration was traceable to STUK [16]. To see if the dose profile from the LIC was similar to the one from CT-SDD2 (2x2) comparable measurements were done. The LIC was placed in a special, 30 cm long PMMA phantom with a diameter of 160 mm that was positioned free in air by using a holder attached to the table i.e. the same phantom that was used in 2.1.2. The center hole was a little bit bigger than in standard phantoms so that the slightly larger LIC would fit in it. The scan parameters were 120 kV and 200 mA on a GE LightSpeed VCT, Milwaukee, USA, at Norrlands University Hospital in Umeå. A helical scan was made with 40 mm beam collimation and pitch 0.984. The LIC was replaced by CT-SDD2 (2x2). Some extra PMMA was put around it so that it would fill the bigger hole. A helical scan with the same scan parameters was made. The dose profiles peak values were normalized to 1 for comparison.

2.2.3 Angular dependence

To study the angular dependence of the CT-SDD2 (2x2) it was placed in a rotation table under an x-ray tube in an x-ray laboratory at the Department of Radiation Physics at Göteborg University (Figure 9 b)). During all the measurements the settings were 117 kV and 5 mAs. The field from the x-ray tube was set to almost 20x20 cm^2 across the detector and a filtration of 2.5 mm Al was used. The rotation table was controlled with a computer and could turn in steps of one percent of a degree. The study was made by irradiating the probe from -27 degrees to +24 (Figure 9 c)) degrees in steps of 3 degrees except near zero where steps of one degree at a time were used. The angular dependence for the pencil ion chamber was also examined in the same way (Figure 9 a)). A measurement with a field of 5x5 cm^2 was also made on the pencil ion chamber to observe how much that would influence when the whole chamber was not irradiated.

The CT-SDD2 was known to have a big angular dependence because of the back plane. To compare this with the CT-SDD2 (2x2) similar angular measurements were done. Only the field and the filtration were changed to approximately 5x5 cm^2 and 7 mm Al. A measurement with 10 mm Al was also made with the CT-SDD2 (2x2) to observe how the filtration influenced the angular dependence. All measured signals were normalized to one at 0 degrees.

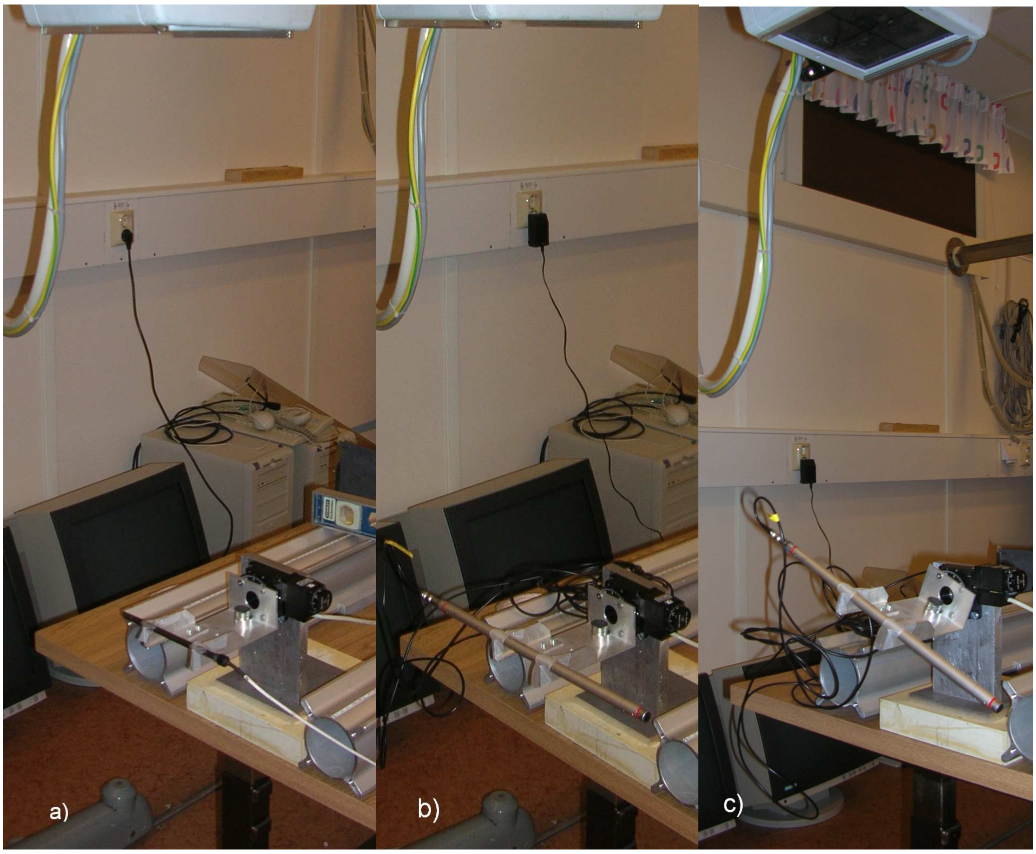

Figure 9: Angular dependence measurements on a) the pencil ion chamber, b) the CT-SDD2 (2x2), c) the CT-SDD2 (2x2) with a large angle.

2.2.4 Rotation symmetry of the detector

In order to observe the rotation symmetry the CT-SDD2 (2x2) and CT-SDD2 were placed in a CT simulator under an x-ray tube in a x-ray laboratory at RTI Electronics AB (Figure 10).

Figure 10: The CT-SDD2 (2x2) in the CT simulator

The CT simulator was a rebuilt watchmaker's lathe that could rotate the probe along its longest axis. The detectors were slowly rotated approximately three whole rotations while the tube was irradiating. The slow rotation (due to limitations of the construction of the CT simulator) caused long exposure times and hence the fluoroscopy mode was used with a low current of about 3 mA. The software "CT-SD16 1906" was used to find the maximum measured value and the minimum measured value.

2.3 Dose underestimation

The CT-SDD2 can measure the whole dose profile. It then measures the whole CTDI and not only $CTDI_{100}$. The amount of radiation inside $CTDI_{100}$ is obviously an underestimation of the dose compared to the total CTDI when it is measured in a phantom. With the software "CT-SD16 1906" any length X of CTDI, $CTDI_X$, can be studied, not only 100 mm as for $CTDI_{100}$. A quotient between $CTDI_X$ and $CTDI_{100}$ is defined as the Scatter $Ratio_X$ and describes the ratio of dose detected inside $CTDI_X$ that is missed by $CTDI_{100}$ if X >100 mm.

$$Scatter\ Ratio_X = \frac{CTDI_X}{CTDI_{100}} \qquad (16)$$

The Scatter $Ratio_X$ is obtained in "CT-SD16 1906" after a measurement and if X has the same length as the whole dose profile $CTDI_X$ is equal to CTDI. This case is called the total Scatter Ratio and is the largest dose underestimation.

2.3.1 Underestimation of dose with $CTDI_{100}$

To see how much the dose is underestimated by $CTDI_{100}$ compared to the whole CTDI, measurements were performed with the CT-SDD2 (2x2) positioned in the central hole of a head phantom. The standard head phantom was placed in a neck support and helical scans were made (Figure 11). The voltage was 120 kV and the current was 200 mA. Measurements were made with 5, 10, 20 and 40 mm beam collimation and the pitch was 1 for 5 and 10 mm beam collimation, 0.969 for 20 mm beam collimation and 0.984 for 40 mm beam collimation. The measurements with 5 and 10 mm beam collimation were made on a Siemens Somatom Plus 4 Power, Erlangen, Germany, and the measurements with 20 and 40 mm beam collimation were made on a GE LightSpeed VCT, Milwaukee, USA, both at SU in Göteborg. At least two measurements per examination were made. The total Scatter Ratio was received and compared.

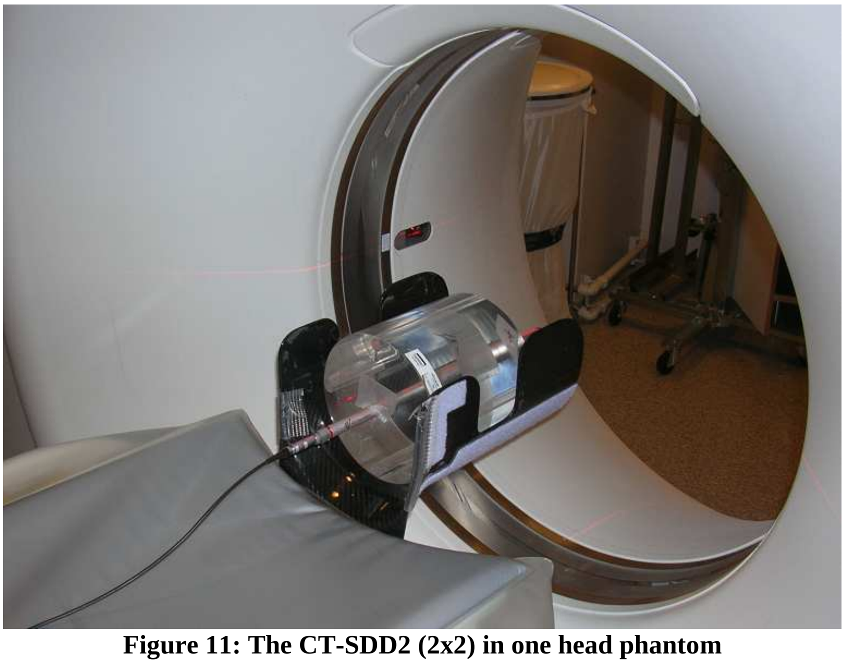

Figure 11: The CT-SDD2 (2x2) in one head phantom

2.3.2 Underestimation of dose with only one head phantom

To observe if the length of the head phantom affects the Scatter Ratio two head phantoms were placed very closely together in the neck support in a GE LightSpeed VCT, Milwaukee, USA, at SU in Göteborg (Figure 12). The detector CT-SDD2 (2x2) was placed 10 mm from the joint between the two phantoms. Helical scans were made over both phantoms with 20 and 40 mm beam collimation with a pitch of 0.969 and 0.984 respectively. The scan parameters were 120 kV and the 200 mA. At least two measurements per examination were made for each set of parameters. The received total Scatter Ratio was compared to the total Scatter Ratio from one phantom.

Figure 12: The CT-SD D2 (2x2) in two head phantoms

2.3.3 Scatter Index

If the Scatter Ratio was increasing with increasing number of phantoms, there could be a problem when QA is performed with only one phantom. A proposed way to get around this problem would be to make CTDI measurements with more than one phantom and find a connection between one phantom and several phantoms, which better represents a whole body.

To do this a parameter called Scatter Index was received with the software “CT-SD16 1906”. The Scatter Index was calculated with Equation 17 and is the Scatter Ratio in one phantom with X = 130.

$$Scatter\ Index = \frac{CTDI_{130}}{CTDI_{100}} \qquad (17)$$

$CTDI_{130}$ was the integrated dose over 130 mm. The reason why the width of 130 mm was chosen is because all standard phantoms are either 150 or 140 mm wide. To avoid measuring outside the phantom 130 mm was used to get some margins.

With the measured dose from two CTDI head phantoms a small start of the making of a table coupled to the Scatter Index could be done. The Scatter Index measured with one head phantom at both 20 and 40 mm beam collimation was coupled to the total Scatter Ratio from two head phantoms for 20 and 40 mm beam collimation.

2.4 A new way of QA

There are five holes for a detector in a CTDI phantom, one in the center and four in the periphery. By measuring the $CTDI_{100}$ with single axial scans in the middle of the pencil ion chamber in all the holes the $CTDI_w$ can be calculated with Equation 5.

When measurements are done with the CT-SDD2 (2x2) in the central hole of a phantom there is the same amount of attenuating material around the detector in all directions in the x-y-plane. This means that it does not matter if the x-ray tube irradiates for example under or over the detector during its helical path around the phantom (except for some small attenuation in the table). If the probe is placed in a peripheral hole there is a big difference in attenuating material in different directions. That can be a problem for measurements with helical scans. Certain pitch-values must be used to be able to measure the dose correctly in the peripheral holes [17]. Not all CT systems have the function to choose pitch freely and the pitches that can enable correct measurements in the peripheral holes are quite uncommon. This means that the probe can not measure the dose in the peripheral holes for all CT systems and hence not the $CTDI_w$, $CTDI_{vol}$ and DLP.

It is impossible to measure in the peripherial holes with the CT-SDD2 due to the present correction made for the back plane.

A way to get around this problems would be if it was possible to get a CTDI factor k to multiply $CTDI_{100,c}$ with to get the $CTDI_w$.

$$k = \frac{CTDI_w}{CTDI_{100,c}} \qquad (18)$$

The CTDI factor k could be established by doing the measurements in all the holes with the pencil ion chamber once.

If k was known for a certain CT system it would be possible to calculate $CTDI_w$, $CTDI_{vol}$ and DLP after only one helical scan i.e. $CTDI_{100,c}$. This would be the case for measurements using the CT-SDD2 (2x2)and the CT-SDD2 as well as the ion chambers.

2.4.1 CTDI factor k for different CT systems

$CTDI_w$ is measured at CT QA. To see if the CTDI factor k was similar for different CT systems, protocols from earlier yearly QA on CT systems at SU in Göteborg were examined. For all the protocols, where a head phantom and the scan parameters 120 kV and 200 mA were used, the CTDI factor k was calculated. The only parameter that was different on some of the CT systems was the scan field of view (SFOV). The SFOV determines which bowtie filter that is used. Different filters are used for body and head.

2.4.2 Axial scans over the CT-SD16 to get CTDI factor k?

A test to see if it was possible to obtain the same CTDI factor k with the CT-SD16 (S/N: 0601009) in the same way as for the pencil ion chamber, the probe was placed in the central hole of the CTDI head phantom and a single axial scan was made on the detector in a Siemens Somatom Plus 4 Power, Erlangen, Germany, at SU in Göteborg. This was a “point dose” measurement and not a $CTDI_{100}$ measurement as for the pencil ion chamber. The CT-SD16 was moved to a peripheral hole and a new single axial scan was made on it. Identical measurements were done in all the peripheral holes. The voltage was 120 kV, the current was 200 mA and the collimation was 10 mm. A dose template in the software “CT-SD16 1906” was used to get a signal. CTDI factor k was calculated by using the signal as $CTDI_{100,c}$ and $CTDI_{100,p}$ in Equations 4 and 18.

For the pencil ion chamber the CTDI factor k was calculated from the standardized CTDI measurements using Equations 4 and 18. The same mA and kV as for the CT-SD16 were used.

3.1 Dose profile acquired by helical scans and axial sequential scans respectively

A derivation illustrating that it is possible to measure the same dose profile using helical scan mode as using axial sequential scan mode was received successfully. It showed that the dose inside the 100 mm that marked $CTDI_{100}$ had to be multiplied with the pitch (Equation 14) for helical scans.

The dose profiles from helical scans and axial sequential scans were compared and the helical scan had a slightly lower dose (0.9 %) in the peak (Figure 13). The area under the helical measured dose profile differed with 1.02 % compared to the one measured with axial sequential scans.

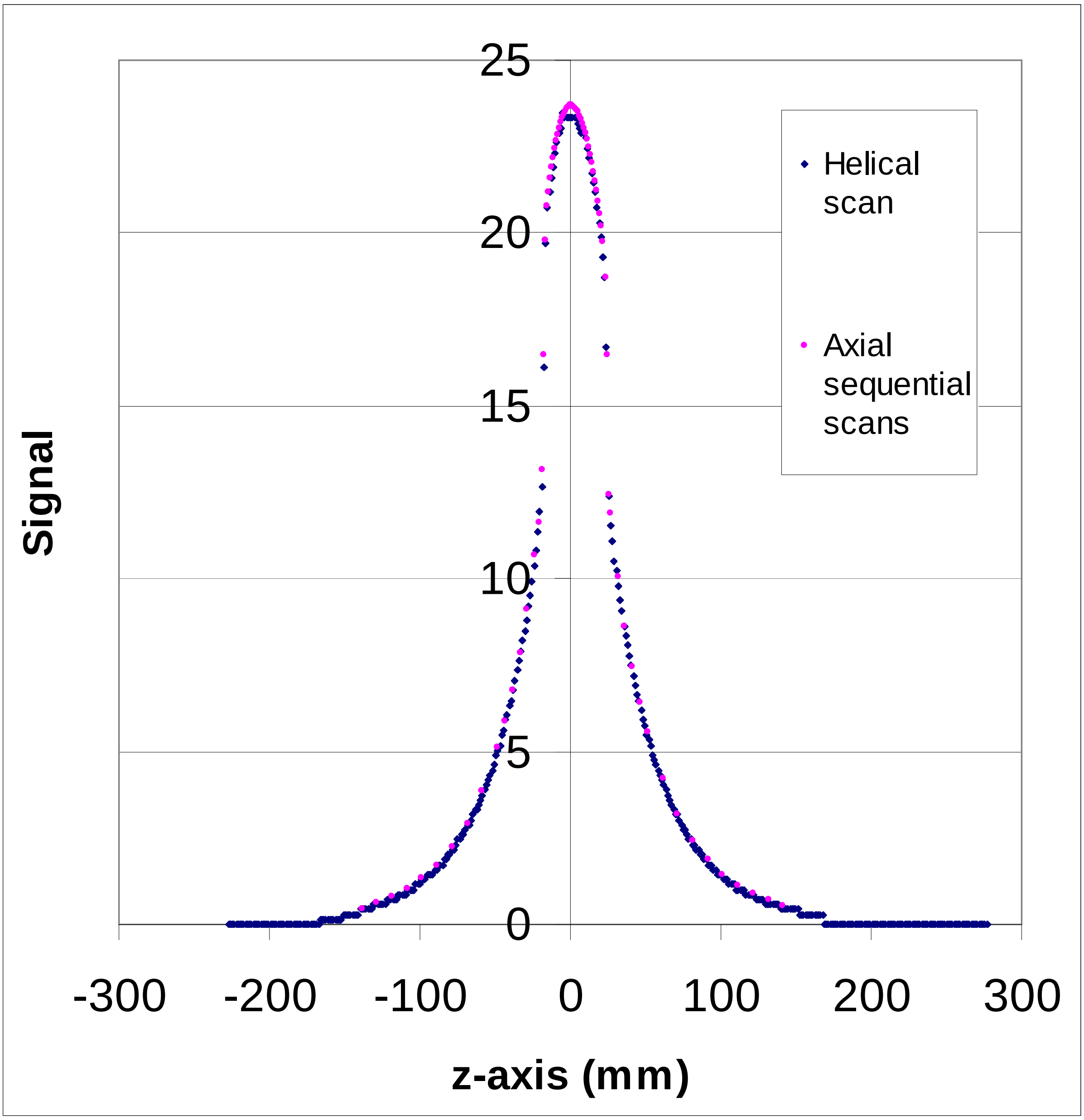

Figure 13: Dose profiles acquired by a helical scan and by axial sequential scans measured with CT-SDD2 (2x2). The scan parameters were 120 kV, 200 mA and 40 mm collimation.

3.2 Results from the evaluation of CT-SDD2

3.2.1 CT-SDD2 versus CT-SDD2 (2x2)

The correction for the CT-SDD2 due to the back plane (1.3) was made so that it could be compared with CT-SDD2 (2x2) (Figure 14). The tails in the corrected dose profile were very symmetrical which indicates that the correction was good.

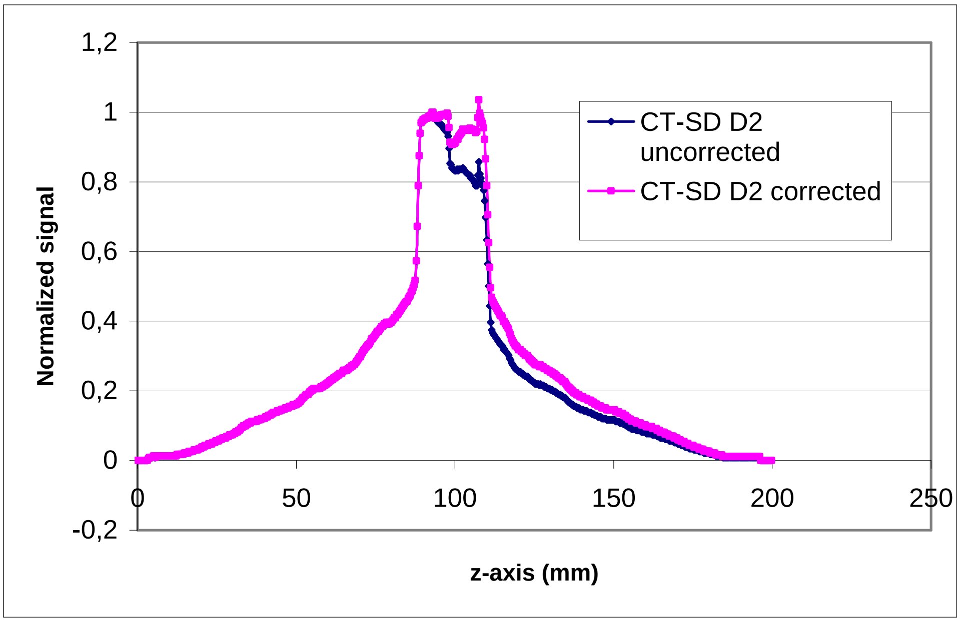

Figure 14: Dose profiles from the CT-SDD2, uncorrected and corrected. The scan parameters were 120 kV, 200 mA and 10 mm collimation.

The tails of the dose profiles measured with helical scans for the both detectors showed good agreement (Figure 15). The disagreement in the peak is the result of the neck support that affected the dose profiles in different positions which made the two independent scans hard to compare exactly.

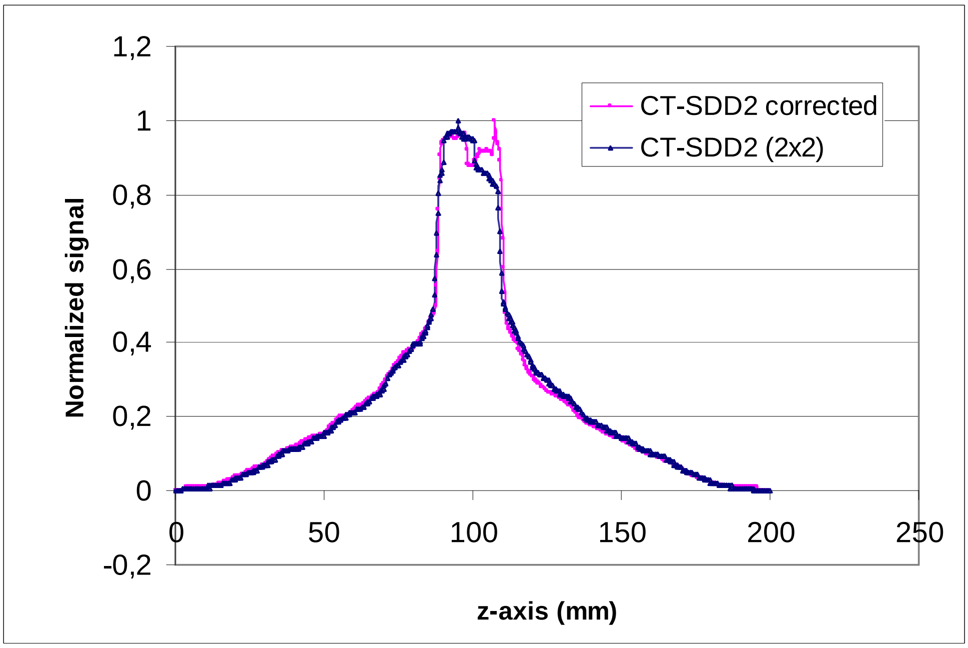

Figure 15: Illustrates the dose profile from the CT-SDD2 and CT-SDD2 (2x2) normalized to a peak value of 1. The scan parameters were 120 kV, 200 mA and 10 mm collimation.

3.2.2 The CT-SDD2 (2x2) versus the LIC

The dose profiles from the CT-SDD2 (2x2) and the LIC were normalized to a peak value of 1 (Figure 16). The area under the dose profile measured with the CT-SDD2 was 1% smaller than the one measured with the LIC and the dose profiles agreed well.

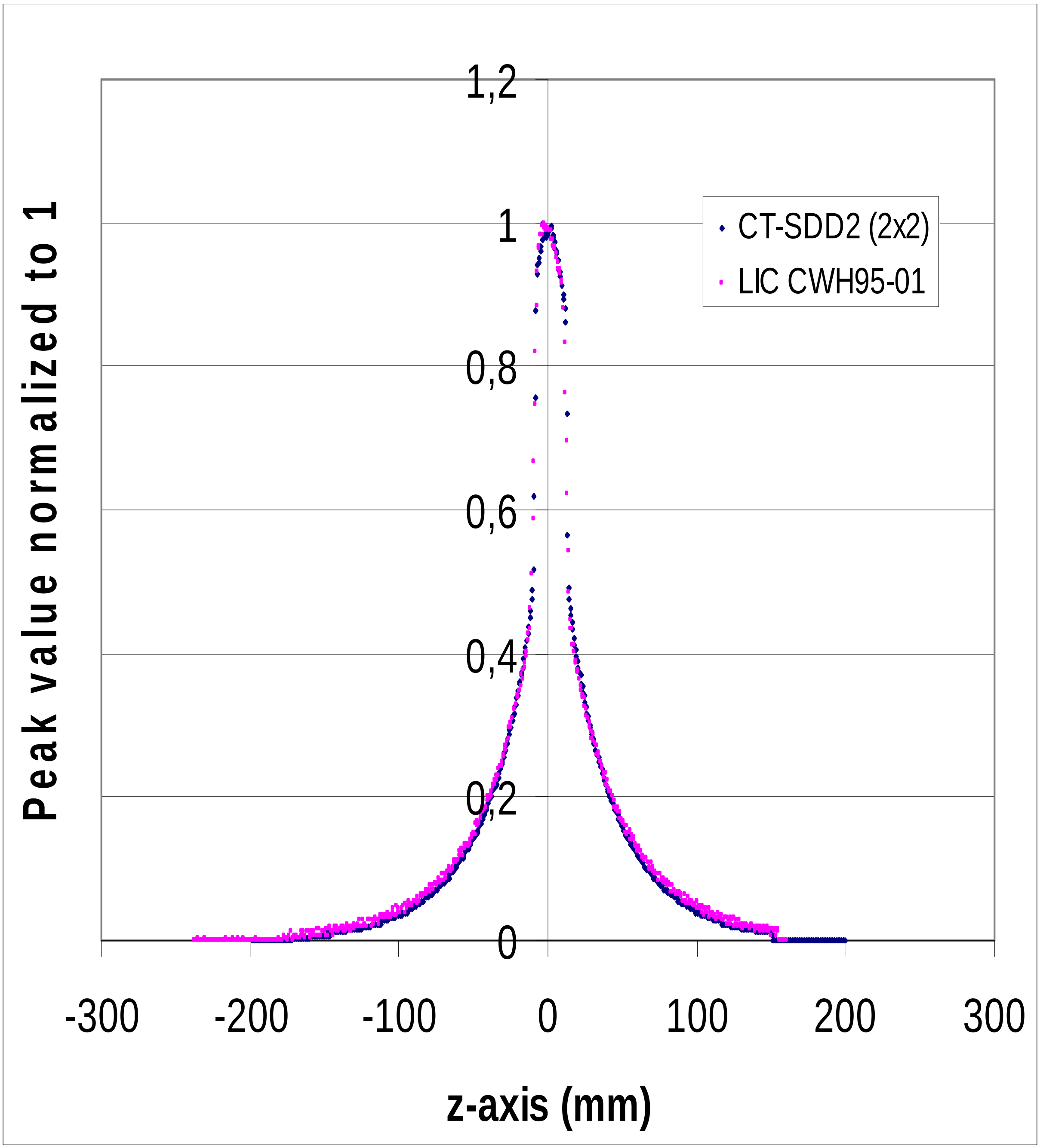

Figure 16: Dose profiles from the LIC and the CT-SDD2 (2x2) normalized to a peak value of 1.

3.2.4 Angular dependence test

The measured signal with CT-SDD2 (2x2) was 5-6 % lower at 0 degrees than at ±20 degrees for a 20x20 mm^2 field and a filtration of 2.5 mm Al (Figure 17 a)). At 0 degrees the smallest possible area of the detector was pointing in the direction of the radiation. The pencil ion chamber was not affected by the different angles for a 20x20 cm^2 field (Figure 17 b)).

When the field was 5x5 cm^2 the pencil ion chamber had an angular dependence of similar to the CT-SDD2 (2x2) at 20x20 cm^2.

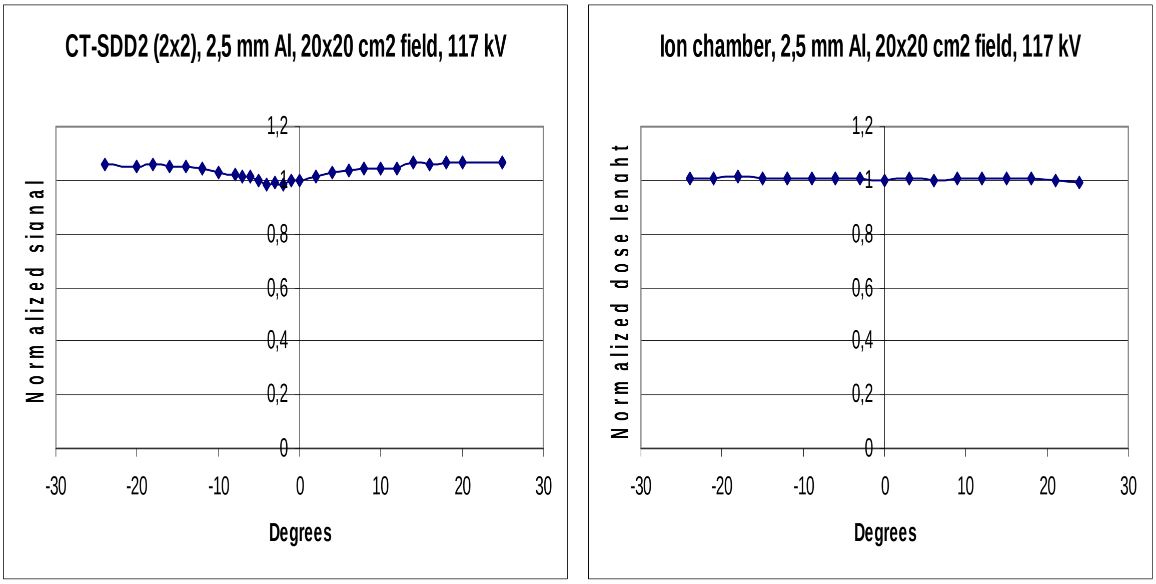

a b

Figure 17: a) The angular dependence for the CT-SDD2 (2x2) and b) the pencil ion chamber

The measured signal with CT-SDD2 (2x2) was 4-5 % lower at 0 degrees than at ±20 degrees for a 5x5 mm^2 field and a filtration of 7 mm Al (Figure 18 a)). When the filtration was changed to 10 mm Al, the difference in signal from 0 degrees to ±20 degrees was 3-4%. The angular dependence for CT-SDD2 (2x2) seamed to be smaller with harder filtration.

There was a large angular dependence of the CT-SDD2 witch shows the importance of the correction in the software (Figure 18 b)).

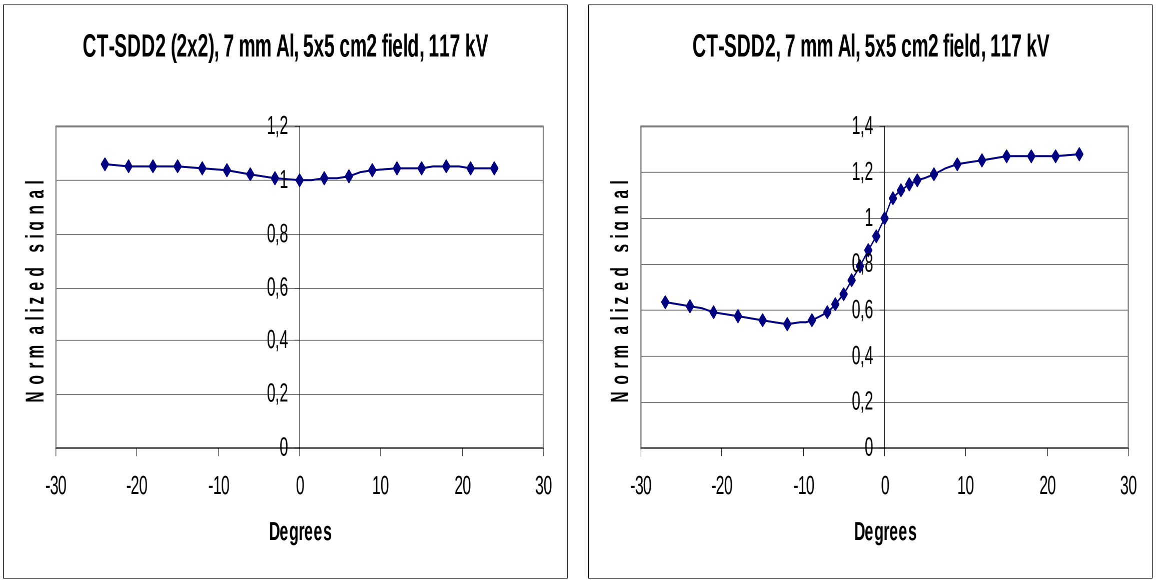

a b

Figure 18: a) The angular dependence fore the CT-SDD2 (2x2) and b) the CT-SDD2

3.2.5 Rotation symmetry

The result from the measurement with the rotating probe under a constant radiation field is illustrated in figure 19 for CT-SDD2 (2x2) and in figure 20 for CT-SDD2.

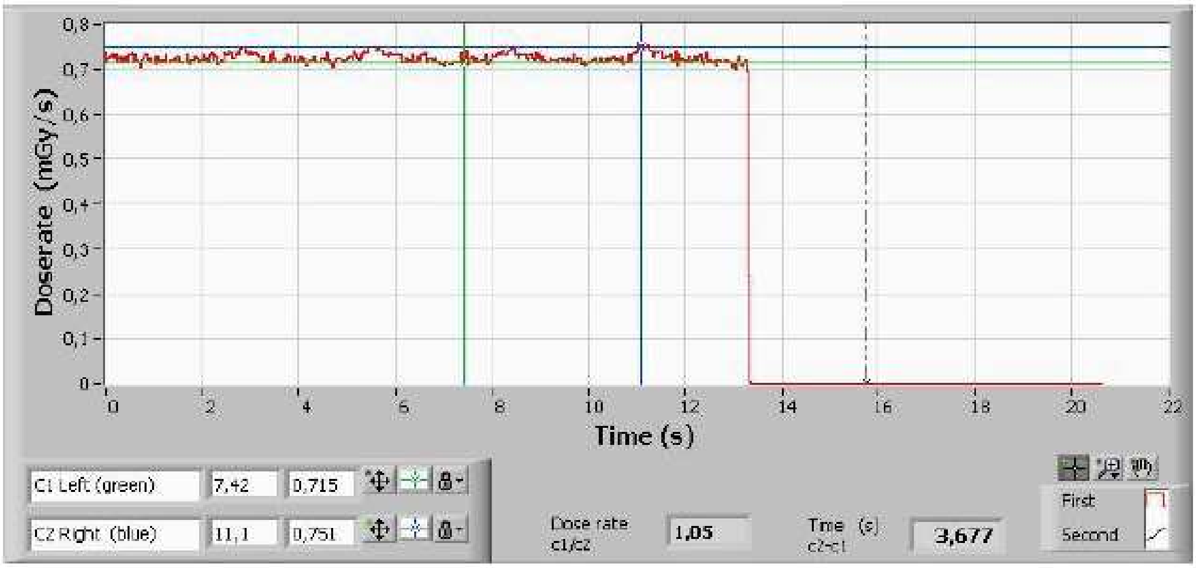

Figure 19: The detected signal during three rotations of the CT-SDD2 (2x2)

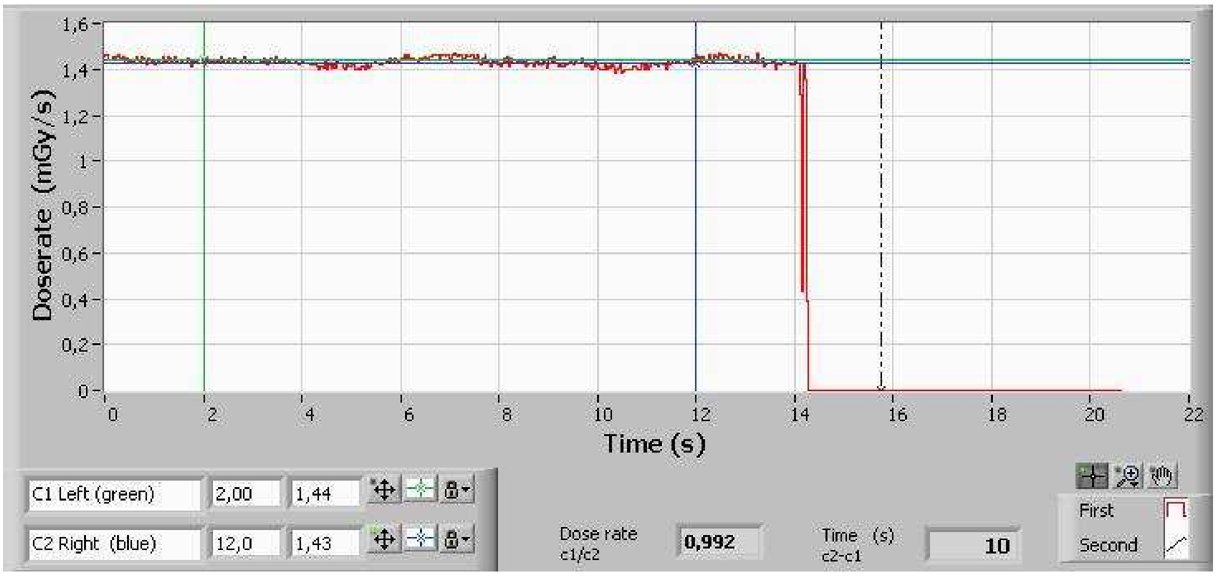

Figure 20: The detected signal during three rotations of the CT-SDD2

The rotation symmetry of CT-SDD2 (2x2) and CT-SDD2 differed at the most with ±2.5 %. The very low signal level of 3 mA, compared to normal levels of 200-400 mA, resulted in visible inherent detector and electrometer noise.

3.3 Underestimation of dose

3.3.1 Underestimation of dose in a head phantom

After a measurement over the head phantom a dose profile was plotted in the software "CT-SD16 1906". The CTDI, $CTDI_{100}$, FWHM, Scatter Index and Scatter Ratio were received (Figure 21). The dip in the top of the dose profile was due to the table attenuation.

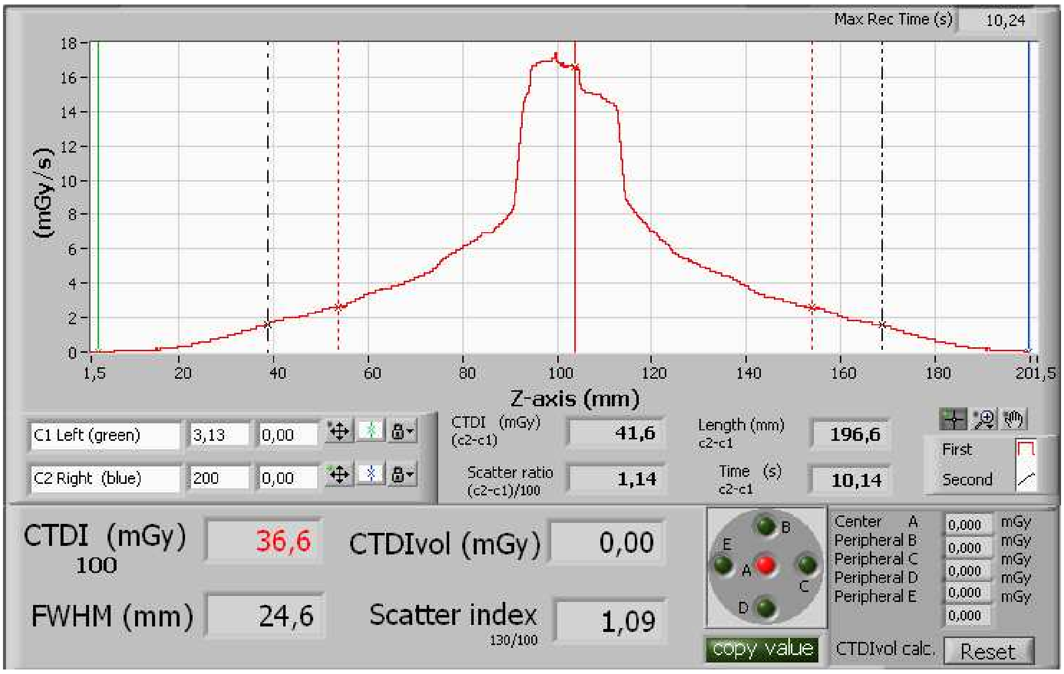

Figure 21: Dose profile, CTDI, $CTDI_{100}$, FWHM, Scatter Index and Scatter Ratio for one head phantom with 20 mm collimation. $CTDI_{100}$ was between the red dotted lines and the whole CTDI was between the green and the blue cursors.

The total Scatter Ratio values for different beam collimations with one or two phantoms are presented in Table 1.

Table 1: The scatter radiation measured in one and two phantoms for different beam collimations.

Number of phantoms	Collimation (mm)	Average total Scatter Ratio	Scatter Index	Number of measurements
1	5	1.14	1.09	2
1	10	1.14	1.09	5
1	20	1.14	1.09	2
1	40	1.16	1.09	2
2	20	1.27	1.09	2
2	40	1.28	1.10	2

For 5 to 20 mm beam collimation in one head phantom the average total Scatter Ratio was 1.14, which means that the dose was underestimated by 12.3 % with $CTDI_{100}$ compared to CTDI. At 40 mm beam collimation the dose was underestimated by 13.8 %. When two head phantoms were used the total Scatter Ratio was increasing even more for 20 and 40 mm collimation and $CTDI_{100}$ underestimated the total dose by 21.3 and 21.9 % respectively. The software only used two decimals for the Scatter Ratio so there was no detectable difference between the many measurements that constituted the average Scatter Ratio.

3.3.2 Scatter Index

The Scatter Index for one head phantom was 1.09 for the CT GE LightSpeed VCT, Milwaukee, USA, for all beam collimations and is shown together with the Scatter Ratio in Table 1. For two head phantoms the Scatter Index was almost unchanged.

3.4 The CTDI factor k

The results from old CT protocols from QA performed in Göteborg from the year 2000 to 2007 are presented in table 2. The CTDI factor k was around 1 for the CT systems from GE, around 1.075 for CT systems from Siemens and Philips and around 1.04 for the CT system from Toshiba.

Table 2: Lists k in a CTDI-phantom for different CT models

CT model	SFOV	kV	Average CTDI factor k	Standard deviation	Number of measurements
GE LightSpeed Pro 16	25	120	0.983	-	1
GE LightSpeed Ultra, 8 slice	25	120	0.996	0.002	6
GE LightSpeed 16 Pro	25	120	0.998	0.009	3
GE LightSpeed VCT	25	120	1.024	-	1
Siemens Somatom Plus 4 Power	50	120	1.066	0.011	6
Siemens Somatom Sensation 16	50	120	1.088	0.005	5
Toshiba Aquilion 16	na	120	1.040	0.007	3
Philips Brilliance 40	50	120	1.077	-	1

Single axial measurements were done over the CT-SD16 to test if a factor k could be calculated from the signals. The dose rate variation during one rotation from the measurements in the central and the peripheral holes was very different. In the central hole the dose rate variation was affected by the same amount of PMMA in all directions and the difference in amplitude was only depending on the neck support (Figure 22 a)). For the peripheral holes the amount of PMMA was changed in all directions so the dose rate variation got a high amplitude when the thinnest part of the phantom was irradiated and low amplitude when the thickest part of the phantom was between the detector and the x-ray tube (Figure 22 b)).

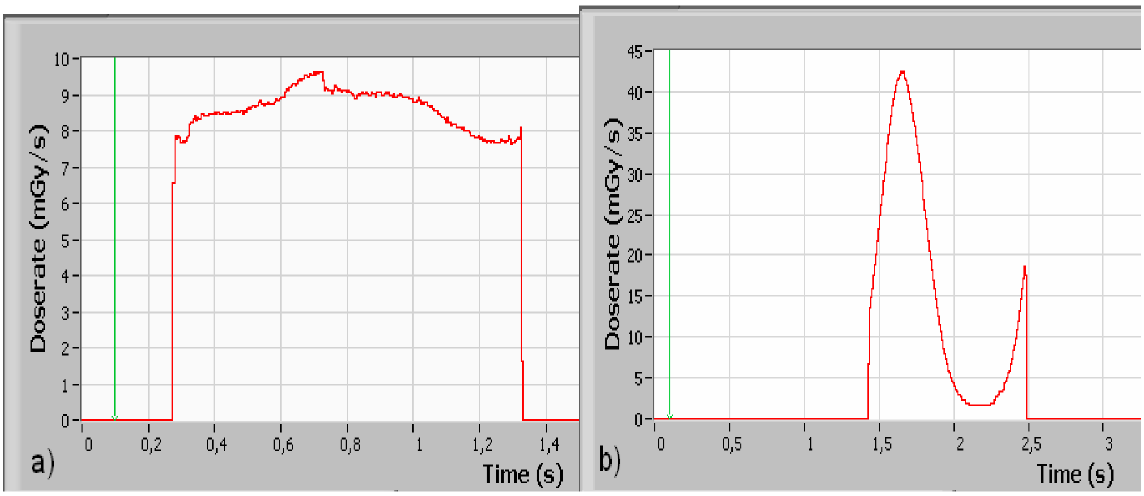

Figure 22: Dose rate variations measured with single axial scan with the CT-SD16 in a a) central hole and a b) peripheral hole.

The calculated CTDI factor k was 1.61. For comparison the CTDI factor k was also calculated using measurements with a pencil ion chamber. The result was 1.08. The doses measured in all the holes in the head phantom with the pencil ion chamber were almost identical. With the CT-SD16 the signal in the center hole was half the value of the signal in the peripheral holes. Hence the test showed that it was not possible to receive the CTDI factor k with this method for CT-SD16.

4. Discussion

4.1 Axial sequential scans versus helical scans

It was shown that the dose profile could be measured with both axial sequential scans and helical scans theoretically. The reason why the dose profile measured with a helical scan was a little bit lower than the one made with axial sequential scans could be due to a combination of low signal resolution and the sampling speed for the helical scan.

The detector electrometer integrates the dose rate signal each 0.5 ms with a dynamic range of 20 bits for each sample. When the template in the software "CT-SD16 1906" for CTDI measurements was used the 20 bits is scaled down to the most valid 8 bits for the wave form data that is used to plot the dose profile. For the dose template, the dynamic range of 20 bits is kept hence the number of discrete values that the signal can take were different for the both measurements. The discrete steps could easily be seen at the tails of the dose profile measured with a helical scan (Figure 13). At its peak the same discrete step for many measurements was obtained which made the peak flat compared to the peak measured with axial sequential scans. The measurements with axial sequential scans did not calculate the signal in a point from waveform data, it obtained it from a whole rotation and kept 20 bits resolution. It would have been better if the helical scan was measured with the same signal resolution.

The software "CT-SD16 1906" had a maximum of 640 samples during one scan independent of the scan length. In this measurement a scan length of 800 mm was used. (This does not show in Figure 13 because the long tail with no signal in the end was removed). The distance moved during sampling time t_s became quite long, about 1.26 mm, which smoothed out the signal measured. This was especially shown in the top of the dose profile where the axial sequential scans were sampled in very small steps of 1 mm. Possibly the dose profiles would fit more exact into each other if the number of samples could be increased or the scan length was shortened. Despite this, the result was quite good since the difference between the dose profiles was not more than 1.02 %.

4.2 Evaluation of CT-SDD2

The two probes CT-SDD2 and CT-SDD2 (2x2) measured almost identical dose profiles after the correction was done for the CT-SDD2. The measurements were done in a neck support which affected the dose profile. In order to avoid a jagged profile it would be better to have used a phantom that was free in air instead of positioned in a neck support. Still, the dose profiles were similar. When a scan of a real patent head is done, the neck support is used which makes it illustrative in that sense. The CT-SDD2 is dependent on which direction the probe is moved through the gantry because of the correction. The CT-SDD2 (2x2) is independent of the direction of the scan.

The comparison of the CT-SDD2 (2x2) and the LIC was done using a phantom that was hung from the table. The area under the dose profiles only differed with 1.0 % and the dose profiles looked almost identical. This showed that the dose profile measured with the probe was correct.

Regarding the angular dependence, the CT-SDD2 (2x2) had a signal at zero degrees that was 6 % lower than at ±15 degrees with a filtration of 2,5 mm Al. With a filtration of 7 mm Al the angular dependence was decreasing to 5 % and to 4 % with 10 mm Al. To futher reduce the angular dependence the aluminium shell on the probe could be made a little bit thinner at the position of the detector. The thinner aluminium would not attenuate as much radiation, which could result in a straighter curve in figure 17 a) and 18 a) and there would be less angular dependence. The angular dependence for the CT-SDD2 was quite huge but was already compensated for with a correction in the software. The reason why the pencil ion chamber had an angular dependence for a 5x5 cm^2 field may depend on the possibility that part of the rotation table got into the field for large angles and therefore contributed with scattered radiation. A smaller radiation field should have been used to eliminate that risk, so even for the measurements with the CT-SDD2 and the CT-SDD2 (2x2). With a 20x20 cm^2 field was the rotation table always in the field.

The rotation symmetry was good for the CT-SDD2 (2x2) and the CT-SDD2 which is important for a detector that measures the irradiation from a rotating x-ray tube. The signal was noisy due to the detector and electrometer noise. The method should maybe be changed to one where only one rotation instead of three is done with higher mA and a very stable generator.

It should be noted that the dose profile measurements performed in this work was made by moving the probe and the phantom through the CT. To completely resemble the measurement situation with the pencil ion chamber, only the probe should be moving through the CT while the phantom should be fixed. To what extent the two measurements leads to different dose profiles is not clear, but it can be assumed that since only the multiple-scattered radiation is affected, the difference is not large.

4.3 Underestimation of dose

$CTDI_{100}$ measured in one head phantom with 20 mm beam collimation did not only miss 12.3 % of the dose in CTDI (Table 1), when two head phantoms were used the underestimation was increasing to 21,3 %. Maybe the total Scatter Ratio would increase even more if a couple of body phantoms were placed after the two head phantoms to more correctly simulate a patient. The reason why only head phantoms were used in this work was because a group in Boston, USA, was studying the Scatter Ratio for one and more body phantoms [18].

$CTDI_{100}$ is known to be an underestimated dose value in a phantom. When a CT system only had beam collimation up to 20 mm this underestimation was constant. $CTDI_{100}$ is used to calculate DLP which is a dose parameter that can be used to calculate a broad estimation of the effective dose by multiply DLP with a conversion factor [7]. The conversion factor is specific for different regions of a body and is calculated by Monte Carlo simulations. As long as the underestimation in $CTDI_{100}$ is constant the conversion factor can be used. With a beam collimation of 40 mm the underestimation was not constant any more. A correction in the conversion factor must probably be made to get the correct effective dose for larger beam collimation than 20 mm. More measurement should be made to confirm that this is really true.

It would have been interesting to measure the dose profile in a CT with larger beam collimation than 40 mm but access to such CT was not available.

The Scatter Index was 1.09 for one head phantom for both 20 and 40 mm beam collimation. This means that if a measurement is done with one head phantom on the same CT and the Scatter Index shows 1.09, the total Scatter Ratio is at least 1.27 or 1.28 depending on what beam collimation that was used. This is shown in Table 1.

4.4 A new way of QA

The CTDI factor k for a head phantom was approximately 1 for CT systems using a SFOV of 25 cm. In this case there was no difference between $CTDI_{100}$ and CTDIw. That is not the situation for the body phantom which has another CTDI factor $k > 1$. The CTDI factor k is specific to a certain type of CT and its equipment such as neck support etc. An improvement in the software “CT-SD16 1906” would be to change it so that the scan length, name of the CT system and type of phantom must be chosen before the measurement. A table that contains the CTDI factor k for all CT systems and phantoms can be made and put in the software. It would then be possible to get $CTDI_w$, $CTDI_{vol}$ and DLP after only one measurement. The time consuming process to get the $CTDI_w$, with a lot of running in and out of the examination room, can thereby be reduced. This is not only a method that makes the

QA faster with the probes, it can also be used for the ion chambers. A simulation of how this faster “one shot method” would look like can be seen in appendix B.

The method to get the CTDI factor k using the probes and single axial scans did not work because of the different detector sizes. The 100 mm long pencil ion chamber collected much more scattered radiation in the phantom holes than the 0,3 mm long detector. The pencil ion chamber measured a part of the dose profile and the CT-SD16 measured only the dose in a point so these were not similar measurements after all. The dose and the dose rate variation in a small point in the phantom can however be studied using this method with CT-SD16.

When the energy dependence has been solved it might be possible to get the CTDI factor k from measurements of axial sequential scans in all holes. Until then the CTDI factor k can be received with standard $CTDI_w$ measurements with a pencil ion chamber.

5. Conclusion

In this thesis, two detectors for measurements of dose profile and CTDI were evaluated.

The detectors make it possible to measure a dose profile with a helical scan. The dose profiles measured with the two detectors had the same shape as measured with a calibrated liquid ion chamber. Both detectors had good rotation symmetry. The detector called CT-SDD2 (2x2) was to be preferred because it was not dependent on the direction of the table movement, did not have much angular dependence and can measure in the peripheral holes.

It seems that the amount of underestimated dose in $CTDI_{100}$ is not the same for a beam collimation of 20 mm and 40 mm. Effective doses calculated by DLP for 40 mm beam collimation may not be correct with the present conversion factor.

The software “CT-SD16 1906” may be upgraded so that a table of Scatter Ratio for many phantoms in a row is coupled to the Scatter Index for certain CT systems and phantoms.

With one helical scan the detectors can measure the dose profile, FWHM of the beam collimation, Scatter Ratio and Scatter Index in a head phantom in a CT. Once the energy dependence is known it is also possible to receive CTDI, $CTDI_w$, $CTDI_{vol}$ and DLP with the same helical scan if the special CTDI factor k for the particular CT system is known.

6. Acknowledgments

I would like to thank:

- my fantastic supervisors Lars Herrnsdorf, Simone Eriksson, Magnus Båth and Jonny Hansson for great guidance trough this project.
- everyone in the “x-ray corridor” at the Department of Radiation Physics at SU and everyone at RTI for a pleasant working environment.
- the staff at CT room 15 and 24 at SU in Göteborg for letting me borrow their CT systems
- Jonas Andersson and Love Kull who helped me with the measurements in Umeå.
- EU prodject “MÅL 1” 2006-2007 and Mid Sweden University who built the small PIN diode detector.

7. References

1) Leitz, W., Jönsson, H., *Patientdoser från röntgenundersökningar*. SSI report 2001:01, 2001

2) Linton, O.W., Mettler, Jr, F.A, *National Conference on Dose Reduction in CT, with an Emphasis on Pediatric Patients*, AJR 2003;181:321-329

3) http://www.dagensmedicin.se/nyheter/2007/06/20/varfemtedatortomografigors/index.xml (2007-12-12)

4) *Strålskydd 118, Riktlinjer för remittering till bilddiagnostik* (ISBN 92-828-9460-6) Byrån för Europeiska gemenskapernas officiella publikationer, Luxemburg, 2001

5) Vrieze, T.J, Primak, A., Bruesewitz, M.R, Zhang, J., McCollough, C.H., *CT Dosimetry: A Comparison of Measurement Techniques and Device*, RSNA poster 1249325.qxd, 2006

6) Nagel, H.D (editor), *Radiation Exposure in Computed Tomography*, 4th edition, CTB Publications, Hamburg, 2002

7) Morin, R.L, Gerber, T.C, McCollough, C.H, *Radiation Dose in Computed Tomography of the Heart*, Circulation 2003; 107:917-922

8) http://www.drs.dk/guidlines/ct/quality/mainindex.htm (2007-12-30)

9) Karlsson, H, *Development and evaluation of a new detector and software for measurements of CT dose profile, CTDI and CT tube current variation*, Göteborg University, 2004

10) Herrnsdorf, L., *Initial study of a CT QA-method to determine spatial variation in X-ray focus position (flying focus and collimation) and CT gantry vibrations*, Eur Radiol. Suppl. 2006;16:C-699, Supplement 1.

11) www.rti.se (2008-01-08)

12) Herrnsdorf, L., Björk, M., Cederquist, B. and Mattsson, C., Thungström, G., Fröjdh, C., *Aspect of point dose profile measurement using solid state detector in charactheristic of computed tomography*, 2008, To be published

13) Herrnsdorf, L., Cederquist, B., *A study of energy dependence for a few common used CT chambers and CT slice probes measured in air and in CTDI head and body phantom*, 2008, To be published

14) Wickman, G., *Liquid ionization chambers, on their design, physical properties and practical application.* Umea University medical dissertations. Umea 1991, New series 314-ISSN 0346-6612

15) Johansson, B., *Recombination processes of ions in dielectric liquids. A study of their influence on dosimetry and RBE determination with liquid ionization chambers*. Umea University medical dissertations. Umea 1996. ISSN 0346-6612 487

16) http://www.stuk.fi/asiantuntijapalvelut/mittauspalvelut/kalibrointipalvelut/sv_FI/index/ (2008-01-02)

17) Vrieze, T., Bauhs, J., McCollough, C. *Use of Spiral Scan Acquisitions for CT Dose Measurements: Selection of Optimal Pitch Values to Ensure Reproducible Results*, LL-PH6115-B05, RSNA 2007 (abstract)

18) Lin, P., *CT radiation profile and dosimetry with a small solid state detector with 1, 3 and 5 phantom.* 2008, To be published

Appendix A

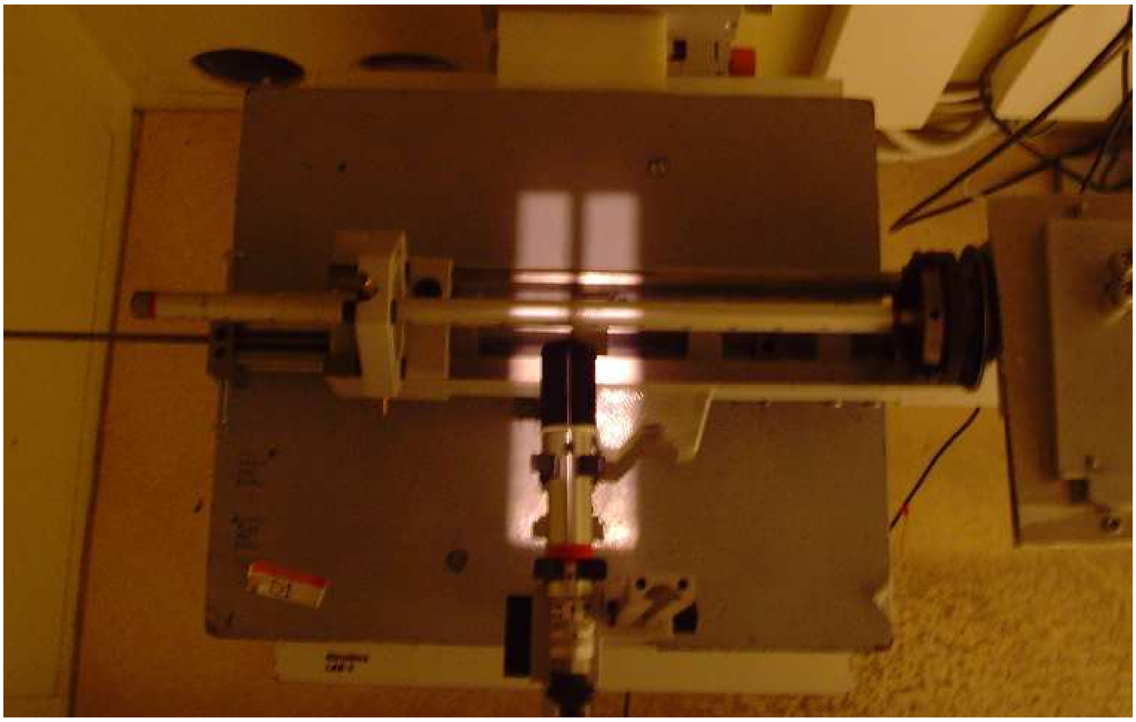

CALIBRATION RECORD

Device: CT-SD16 **Serial number:** DC1-07030063 2x2

Date of calibration: March 19, 2007

Calibration performed by: Mikael Björk

General Information

Scope of calibration: Calibration in terms of air kerma (Ka).

W-value: The reference value of the air kerma as obtained by the primary standard measurements at PTB is based on (W/e)air=33,97 V.
1 Gy = 114,1 R is used to get the R-value .

Climatic conditions: temperature: 23,8 °C pressure: 97,7 kPa

Ref. chamber: Type: Radcal 6cc S/N: 13071
Manufacturer: Radcal
Calibration date: 2005-07-04

Direction of radiation: The detector was irradiated perpendicular to the length of the probe. The cross, marked 0 deg at the detector D2, was directed against the focal spot.

Reference point: 6,5 mm behind the cross at the top marking. The depth is marked with a rim on the detector side.

SDD: 100 ±1 cm

Point of test: In the central beam at the SDD distance.
Dose rate in point of test is 5,0 ±0,2 mGy/s.

Beam quality	Ref. kV	X-ray target	Filtration [1]	HVL in mm Al	N_K in mGy/nC	N_K in mR/nC
RQ RQ	120	Tungsten	2,5 mm Al	4,40	,3818	43,56

1) This is the total filtration including inherent filtration.

The inaccuracy of the calibration factor is less than ±3 %.

RTI Electronics AB, Sweden

Sign:____________________________

Recommended calibration interval is 24 months in accordance with RTI document 5-KA-51025-0, Calibration Routines, Dose and Dose Rate.

Ref. No.: 07-03-30002-00-23656

Appendix B

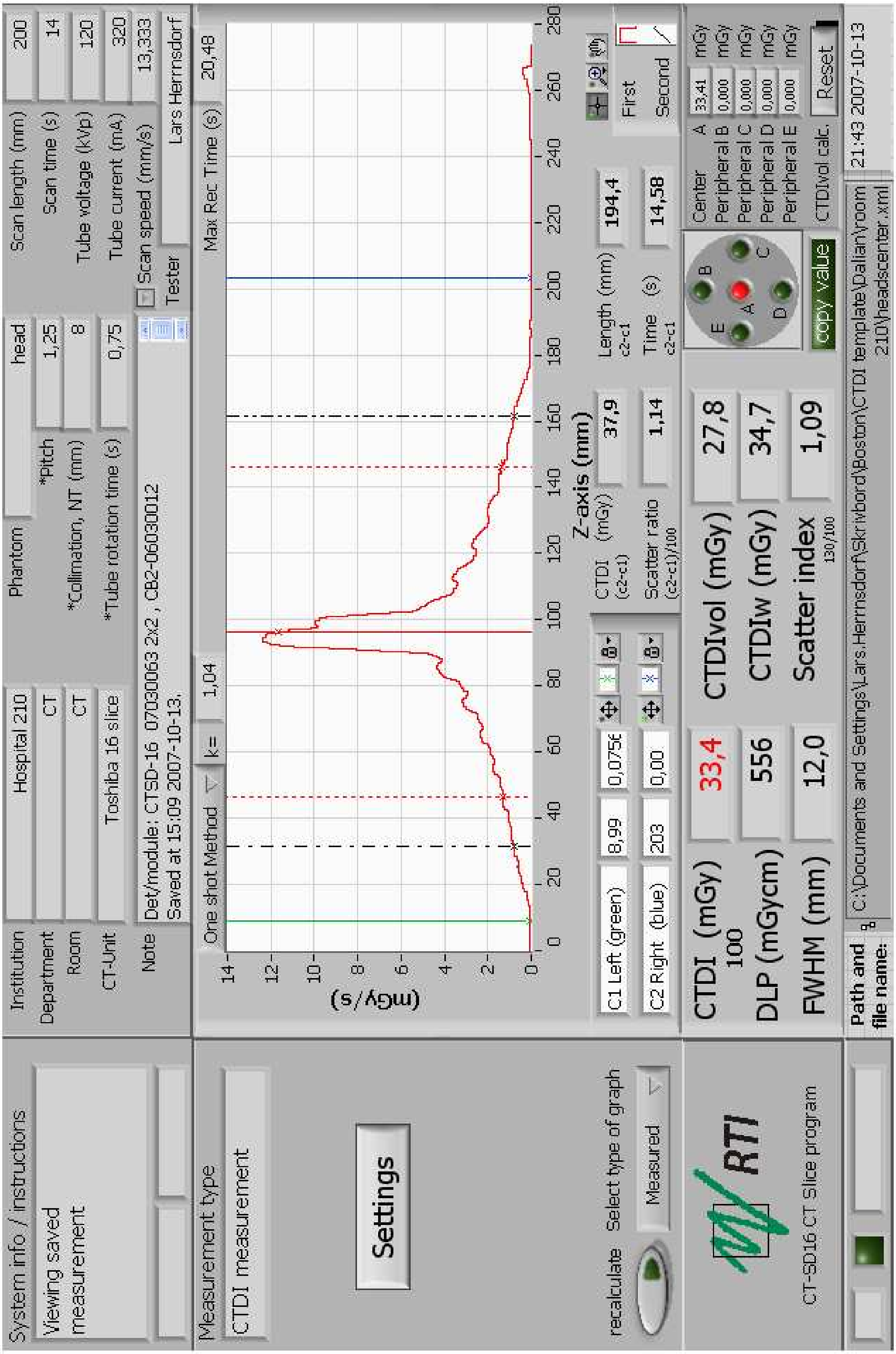

System info / instructions
Viewing saved measurement
Measurement type
CTDI measurement
Settings
recalculate
Select type of graph
Measured
RTI
CT-SD16 CT Slice program
Institution
Hospital 210
Department
CT
Room
CT
CT-Unit
Toshiba 16 slice
Note
Det/module: CTSD-16 07030063 2x2 , CB2-06030012
Saved at 15:09 2007-10-13.
Phantom
head
*Pitch
1,25
*Collimation, NT (mm)
8
*Tube rotation time (s)
0,75
Scan length (mm)
200
Scan time (s)
14
Tube voltage (kVp)
120
Tube current (mA)
320
Scan speed (mm/s)
13,333
Tester
Lars Herrnsdorf
One shot Method
k=
1,04
Max Rec Time (s)
20,48
(mGy/s)
Z-axis (mm)
C1 Left (green)
8,99
0,0756
C2 Right (blue)
203
0,00
CTDI (mGy) (c2-c1)
37,9
Scatter ratio (c2-c1)/100
1,14
Length (mm) c2-c1
194,4
Time (s) c2-c1
14,58
First
Second
CTDI100 (mGy)
33,4
DLP (mGycm)
556
FWHM (mm)
12,0
CTDIvol (mGy)
27,8
CTDIw (mGy)
34,7
Scatter index 130/100
1,09
copy value
Center A 33,41 mGy
Peripheral B 0,000 mGy
Peripheral C 0,000 mGy
Peripheral D 0,000 mGy
Peripheral E 0,000 mGy
CTDIvol calc.
Reset
Path and file name:
C:\Documents and Settings\Lars.Herrnsdorf\Skrivbord\Boston\CTDI template\Dalian\room 210\headscenter.xml
21:43 2007-10-13